Characterization of 15 kV SiC n-IGBT and its Application Considerations for High Power Converters

Arun Kadavelugu, Subhashish Bhattacharya
FREEDM Systems Center
North Carolina State University
Raleigh, NC, USA.

Sei-Hyung Ryu, Edward Van Brunt, David Grider, Anant Agarwal*
Cree, Inc.
Durham, NC, USA.
*Currently, with the US. Dept. of Energy.

Scott Leslie
Powerex, Inc
Youngwood, PA, USA.

***Abstract*—The 4H-SiC n-IGBT is a promising power semiconductor device for medium voltage power conversion. Currently, Cree has successfully built 15 kV n-IGBTs. These IGBTs are pivotal for the smart grid power conversion systems and medium voltage drives. The need for complex multi-level topologies or series connected devices can be eliminated, while achieving reduced power loss, by using the SiC IGBT. In this paper, characteristics of the 15 kV n-IGBT have been reported for the first time. The turn-on and turn-off transitions of the 15 kV, 20 A IGBT have been experimentally evaluated up to 11 kV. This is highest switching characterization voltage ever reported on a single power semiconductor device. The paper includes static characteristics up to 25 A (forward) and 12 kV (blocking). The dependency of the power loss with voltage, current and temperature are provided. In addition, the basic converter design considerations using this ultrahigh voltage IGBT for high power conversion applications are presented. Also, a comparative evaluation is reported with an IGBT with thicker field-stop buffer layer as a means to show flexibility in choosing the IGBT design parameters based on the power converter frequency and power rating specification. Finally, power loss comparison of the IGBTs and MOSFET is provided to consummate the results for a complete reference.**

I. INTRODUCTION

The 6.5 kV Silicon (Si) IGBTs are the highest voltage power semiconductor devices commercially available for high switching frequency power conversion. But, the growing interest in smart-grid power electronics at distribution voltage levels requires the Si IGBTs to be either connected in series or using multi-level converter topologies. The series connection requires expensive snubber circuits for voltage balancing and results in significant power loss [1]. On the other hand, the multilevel topologies need complex controllers and suffer from voltage and power balancing problems [2]. Owing to these problems, there has been a considerable interest to develop high voltages devices (> 10 kV) using SiC [3], [4].

The 10 kV 4H-SiC MOSFETs are viable high voltage devices with low on-resistance while allowing switching frequencies beyond 20 kHz [4]. But, like in the case of Si, MOSFETs are not feasible for higher voltage due to increased drift resistance (due to unipolar nature) which is amplified further with temperature. In [5], it is predicted that approximately above 9 kV, IGBTs are better than MOSFETs, for the same foot-print size. Initially, IGBTs were designed with p-type drift due to practical limitation in preparing low resistivity p-SiC substrates required for the n-IGBTs [6]. However, with advances in the SiC technology, n-IGBTs have also been built [7], [8]. As predicted, the n-IGBTs are superior to p-IGBTs in terms of on-state drop as well as switching characteristics [8].

The following section of the paper reports the performance of the state-of-the-art 15 kV, 20 A, n-IGBT. In Fig. 1, the cross-section of the IGBT is shown. The thicknesses of the field-stop buffer layer and the drift region are 2 µm and 140 µm respectively as shown.

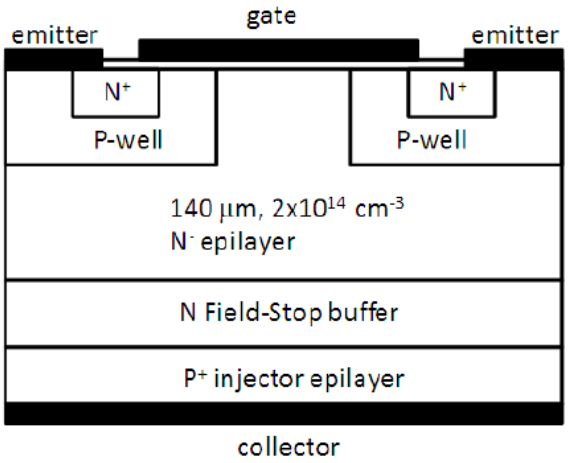

Figure 1: Cross-sectional view of the 15 kV n-IGBT.

This work is supported by ARPA-E Contract #DE-AR0000110.

II. STATIC CHARACTERISTICS

Fig. 2 shows the 15 kV, 20 A, IGBT co-pack module consisting of two series connected 10 kV SiC JBS diodes (effectively 20 kV diode) anti-parallel to the IGBT. The module has integrated current-sense resistors for shoot-thru protection and a thermistor to provide temperature information as shown in the figure.

Fig. 3 shows forward characteristics of the IGBT up to 25 A, at 25°C and 150°C temperature conditions. The on-drop is increasing with temperature making the IGBT inherently suitable for parallel operation. The leakage currents up to 12 kV are shown in Fig. 4, and it is evident that the power dissipation under at 12 kV blocking condition is about 1.8 W, which is practically negligible. The non-linear collector to emitter capacitance, $C_{CE,}$ of the module is shown in Fig. 5, up to 17 V.

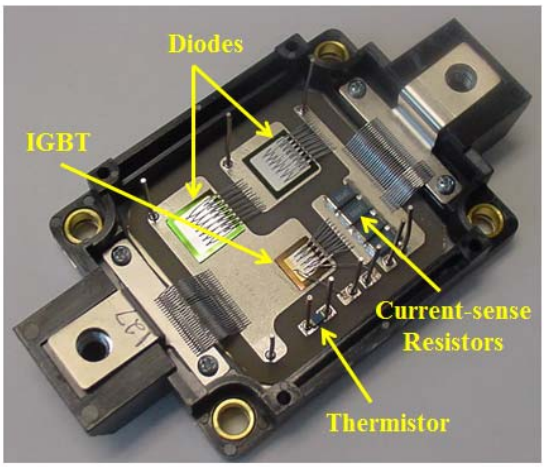

Figure 2: The packaging information of the IGBT co-pack module.

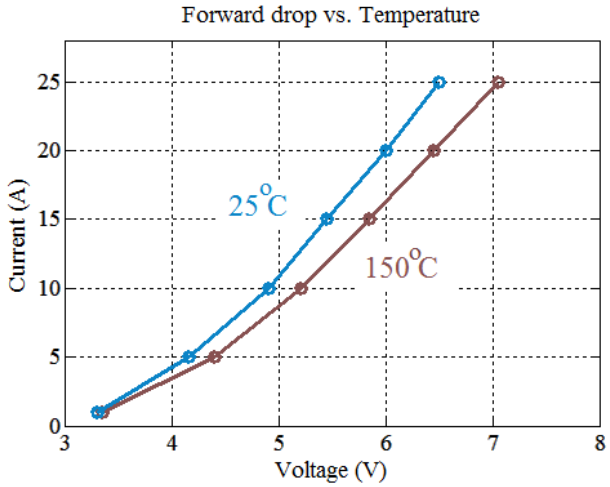

Figure 3: Forward conduction characteristics at 25°C and 150°C (V_{GE} = 20 V).

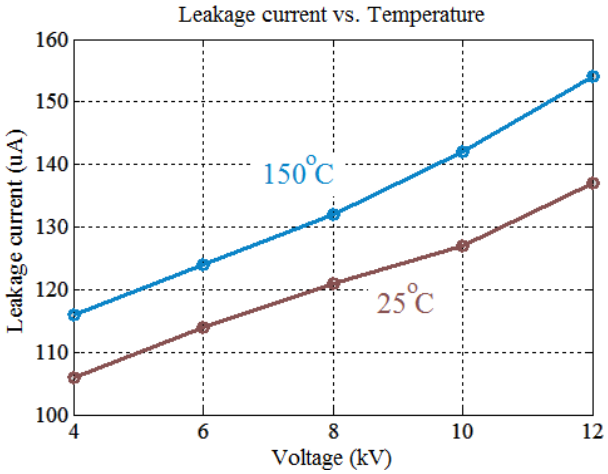

Figure 4: Forward blocking characteristics at 25°C and 150°C (V_{GE} = 20 V).

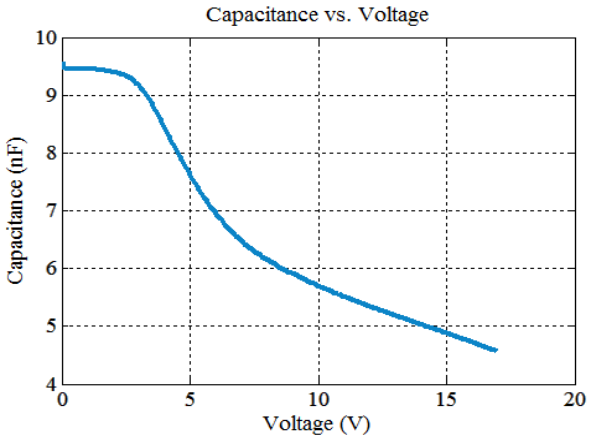

Figure 5: Capacitance, $C_{CE,}$ w.r.t voltage.

III. SWITCHING CHARACTERISTICS

A. 11 kV characteristics at 25°C

The inductive load characteristics of the 15 kV IGBT are evaluated on the double-pulse test circuit shown in Fig. 6. The single layer high voltage load inductor designed for low inter-winding capacitance is shown in Fig. 7. The voltage probe used for measurements is a 20 kV, 75 MHz Tektronix P6015 probe; and the current is measured using a 20 MHz Pearson current monitor. The oscilloscope used for the entire tests is a Tektronix TDS series 500 MHz scope.

Fig. 8 shows the turn-off transition at 11 kV, 10 A under clamped inductive load conditions. The turn-off transient is taking about 650 ns, with a negligible tail time. The turn-off gate resistance, $R_{G(OFF),}$ used is 10 Ω. Unlike, in an ideal inductive turn-off transition, where the current begins to

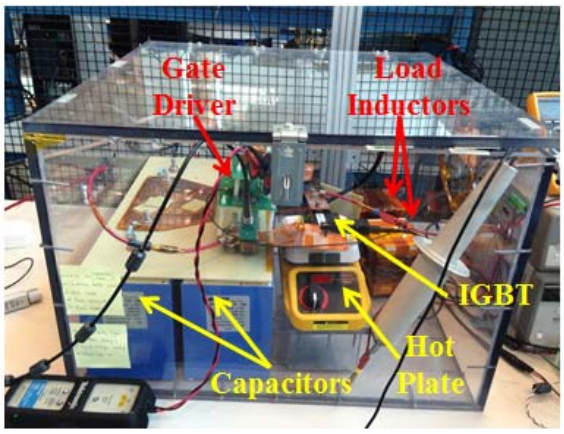

Figure 6: Double pulse tester (rated for 14 kV) used for characterizing the IGBT (High voltage capacitors, IGBT under test, Gate driver, Hot plate and HV Load inductors are shown).

Figure 7: High voltage single-layer load inductor.

drop only after the voltage is raised to the dc-bus value [9], the current here begins to fall slowly before the voltage has reached the DC bus value. This is followed by a sudden fall in the current, once the voltage has reached the DC bus voltage of 11 kV. This is attributed to the partial zero voltage switching (ZVS) [10] turn-off due to the capacitance of the IGBT (C_{CE}) and the diode. The energy loss of the transition is about 18 mJ. The bump in the current is due to decrease in dv/dt, and the consequent reduction of resonant current supplied to the capacitance across the diode.

The turn-on transient at 11 kV, 5 A is shown in Fig. 9. The turn-on transition, unlike in the turn-off transient, has a high current spike and a high dv/dt at the beginning. The current spike shown in the Fig. 9 has a peak value of 39 A. This spike is due to sudden discharging of the capacitance across the diode (current in reverse direction) due to high dv/dt (seen in Fig. 9) by the IGBT attributed to its low depletion capacitance. Once the voltage of the IGBT reaches about 6 kV, the dv/dt is slowed down due to its high diffusion capacitance. This explanation is valid even for the change in slope of turn-off voltage transition shown in Fig. 8.

The oscillation in the current following the spike, during turn-on, is because of resonance between the stray inductance and the capacitance across the diode (that includes capacitance from the load inductor also). To limit the rate of discharge of the depletion capacitance, a high gate resistance is used for the turn-on transition. At 11 kV, to limit the spike to 40 A, the turn-on gate resistance, $R_{G(ON)}$, used is 200 Ω. But this high gate resistance is further slowing down the discharge of the diffusion capacitance also, and thus increasing the duration of the turn-on transition. Consequently, the turn-on loss resulted at 11 kV, 5 A is 52 mJ. At lower voltage (say 8 kV), the $R_{G(ON)}$ value could be significantly reduced which in turn will result in considerably lower loss. It has to be noted that while the turn-off transition was evaluated at 10 A, the turn-on is evaluated 5 A due to limitations from the double-pulse generation circuit and saturation of the load inductor. Also, to further reduce the turn-off loss, it could be attempted to reduce the $R_{G(OFF)}$ from 10 Ω. But this has not been evaluated in this paper. However, as the turn-off transition of the IGBT is primarily dependent on the recombination process, rather than the gate current, the decrease in energy loss with further reduction of $R_{G(OFF)}$ could be insignificant.

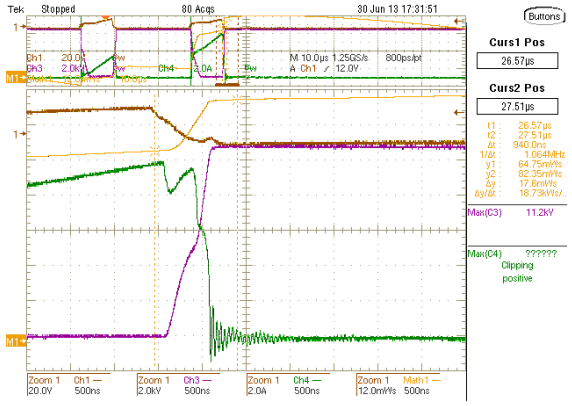

Figure 8: Turn-off transition at 11 kV, 10 A with $R_{G(OFF)}$ = 10 Ω. [Ch1(Brown): V_{GE} – 20 V/div; Ch3(Magenta): V_{CE} – 2 kV/div; Ch4(Green): I_C – 2 A/div; Math1(Orange): Energy loss – 12 mJ/div; Time scale: 500 ns/div].

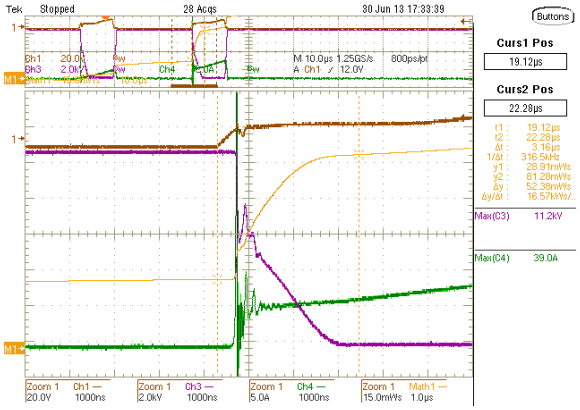

Figure 9: Turn-on transition at 11 kV, 5 A with $R_{G(ON)}$ = 200 Ω. [Ch1(Brown): V_{GE} – 20 V/div; Ch3(Magenta): V_{CE} – 2 kV/div; Ch4 (Green): I_C – 5 A/div; Math1(Orange): Energy loss – 15 mJ/div; Time scale: 1 µs/div].

B. Loss with variation in voltage and current

The IGBT has been tested for dependency of the power loss on voltage and current variation. Fig. 10 summarizes the experimental voltage dependency data. It can be seen that the turn-on loss is almost following the square-law, whereas the turn-off loss is proportionally increasing with voltage. Fig. 11 shows loss variation at 11 kV with change in current. The turn-on loss increased by about 40 % from 3 A to 5 A at 11 kV. The turn-off loss has further weaker dependency on the current. The gate resistances used for all the conditions are same as noted in the previous section, $R_{G(ON)}$ of 200 Ω and $R_{G(OFF)}$ of 10 Ω. Also, the oscilloscope, probes and rest of the experimental setup is same as that used for the earlier section.

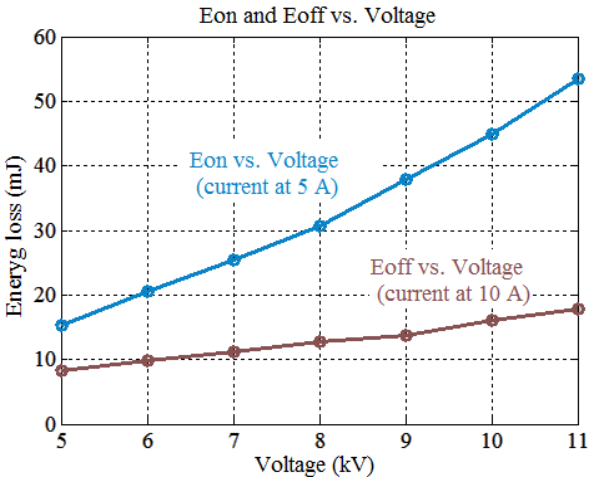

Figure 10: Turn-on and Turn-off loss variation with voltage at 5 A and 10 A respectively.

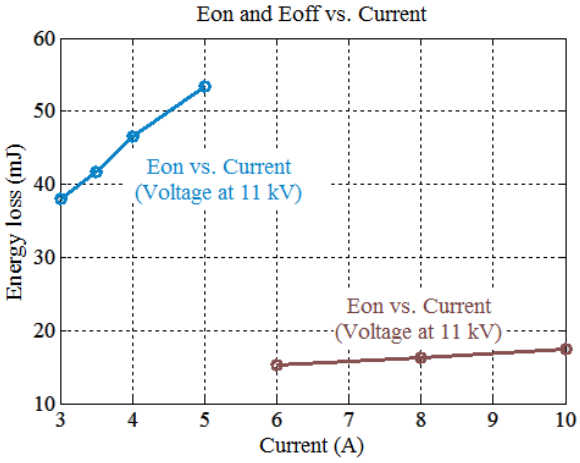

Figure 11: Loss variation with current at 11 kV.

C. Characteristics with temperature variation

The IGBT is characterized from 25° C to 150° C using a hot plate shown in Fig. 6. The experimental waveforms of turn-off transitions at 8 kV, 10 A at different temperatures are shown in Fig. 12. It can be seen that both voltage and current transition times have significantly increased from 25° C to 150° C, and hence the turn-off energy loss also by a factor of 3.2. The increase in turn-off loss with temperature is due to increased carriers in the drift layer, caused by higher lifetime in the field-stop buffer layer, and more injection from the backside. The turn-on loss is practically constant in the entire temperature range of the experiment at 8 kV, 5 A, as shown in Fig 13. This is due to high $R_{G(ON)}$ (used for suppressing the current spike) entirely determining the turn-on loss.

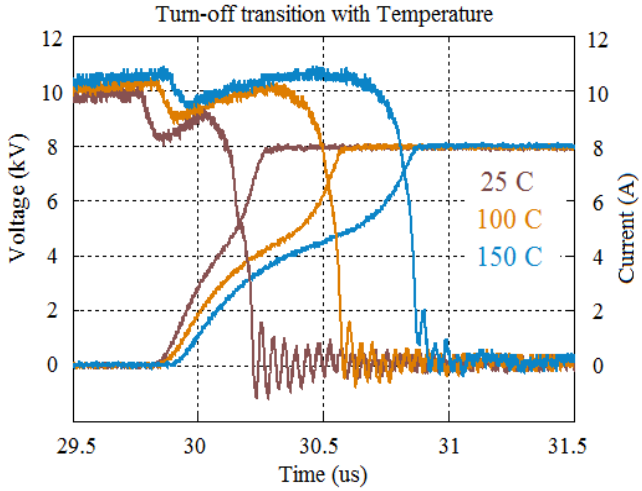

Figure 12: Turn-off loss variation with temperature at 8 kV, 10 A.

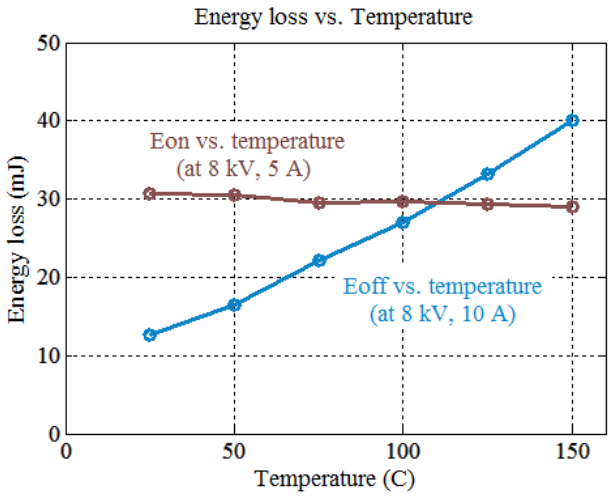

Figure 13: Turn-off and turn-on loss variation with temperature at 8 kV, 10 A and 8 kV, 5 A respectively.

IV. Application Considerations for High Power Conversion

The ultrahigh voltage blocking capability of the 15 kV SiC IGBT makes it a unique choice for medium voltage smart grid and drives applications. The complex multi-level topologies can be replaced with 2-level converters, which drastically reduces the component count and increase the reliability. Also, the challenges of controlling the multi-level converters for voltage and power balancing will be completely eliminated. Moreover, there will no need to generate multiple phase shifted PWM pulses using complex DSP/FPGA integrated controllers. In addition, the size and weight of the power converters are expected to be significantly lower due to lower power loss and high switching frequency capability [3].

But the state-of-the-art 15 kV IGBT also presents some unprecedented challenges for the power converter designers that require careful design and selection of components for developing the power converters. Fig. 14 shows the 11 kV voltage waveform with both turn-on and turn-off transitions. It can be seen that the dv/dt during the beginning of the turn-on transition is high (110 kV/µs) followed by a significantly lower dv/dt (3.3 kV/ µs). As explained earlier, the high dv/dt at the beginning of the turn-on is due to low depletion capacitance of the IGBT. The subsequent phase of slow dv/dt is due to high turn-on gate resistance of 200 Ω used for limiting the high dv/dt (or the current spike) at the beginning of this transition. A similar profile for the dv/dt is also seen from the figure during the turn-off transition as well. But, the dv/dt during the turn-off is not as high as that is observed during the turn-on.

The high dv/dt conditions require a careful design of the gate driver isolation supply. Apart from handling high voltage, the gate driver should be able to handle high dv/dt with minimal injection of common mode currents. Similarly, the converter system should be equipped with di/dt filtering circuits to prevent the electromagnetic interference (EMI) issues due to current spike during turn-on transition.

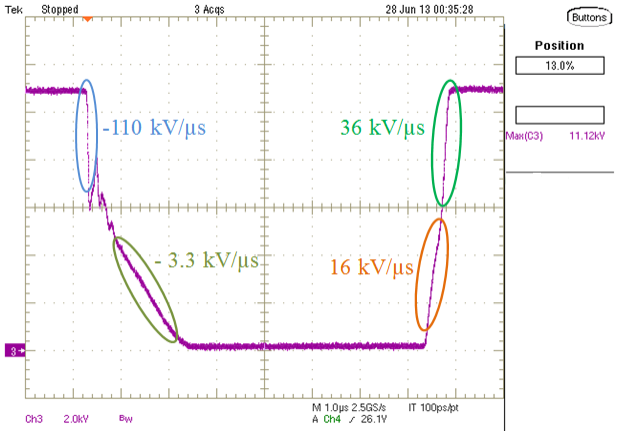

Figure 14: Turn-on and turn-off switching voltage transitions with dv/dt values at 11 kV.

The 200 Ω gate resistance used for turn-on is significantly increasing the duration of the transition. This requires an increase of dead-band period for voltage source converters (VSC). Even in the soft-switched converters, the high dead-band could result in loss of ZVS [11]. This effect is further amplified by the fact that high voltage discharges the resonant inductor at a faster rate.

V. Comparsion of IGBTs with Different Field-stop Buffer Layer Thicknesses

The characteristics presented in sections II and III of the paper are on the 15 kV IGBT designed with a field-stop buffer layer of 2 µm thickness. As shown in [8], the low buffer layer thickness gives advantage of lower on-drop, which is essential for multi-megawatt power conversion systems. On the hand, thinner buffer layer is also responsible for high dv/dt and current spike that are seen during the turn-on transition. The thicker buffer layer IGBT has more conduction loss, but a significantly reduced turn-off transition loss. Also, the dv/dt during the turn-on and the current spike are considerably lower. So, the IGBT parameters have to be appropriately chosen based on the switching frequency and power level requirements of the power converter system.

In this section, a comparative study of the 15 kV, 20 A, 2 µm buffer layer IGBT is done with a 15 kV, 20 A, 5 µm buffer layer IGBT. The IGBTs are identical except for change in buffer layer thicknesses. In [8], a comparative evaluation of 2 µm and 10 µm IGBTs is presented. But the major focus was on turn-off behavior. In this paper, both turn-on and turn-off waveforms are provided for 2 µm and 5 µm devices along with their comparison. Fig. 15 shows forward characteristics of the 15 kV, 20 A, 5 µm buffer layer IGBT with temperature. On comparing with the characteristics of the 2 µm IGBT (shown in Fig. 3), the on-drop at 20 A is 6 V and 7.2 V at room temperature for the 2 µm and 5 µm IGBTs respectively.

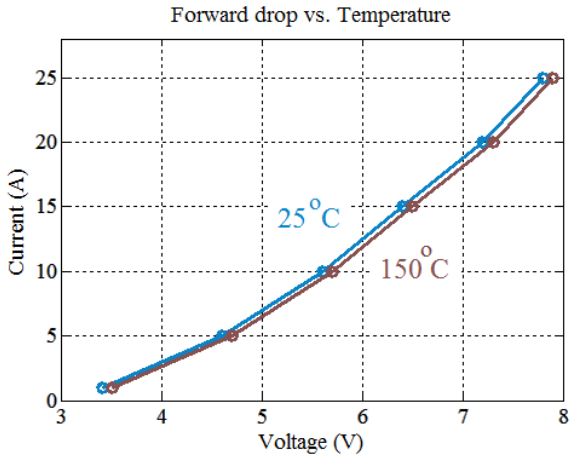

Figure 15: Forward characteristics of 5 µm IGBT with temperature at V_{GE} = 20 V.

The switching loss, dv/dt and current spike of the 5 µm IGBT have been experimentally evaluated at 8 kV and compared with the data of 2 µm IGBT. Fig. 16 and Fig. 17 show turn-on transitions of the 2 µm and 5 µm IGBTs respectively at 8 kV and 5 A. The corresponding turn-off transitions at 8 kV and 10 A for the 2 µm and 5 µm IGBTs are shown in Fig. 18 and Fig. 19 respectively. The turn-off power loss of the 5 µm IGBT is about 50 % of what is observed with the 2 µm IGBT. This is due to lesser injection in the 5 µm IGBT. Table I summarizes the comparison of the IGBTs. The same turn-on loss for both the IGBTs is again due to the dominant effect of the high $R_{G(ON)}$. Also, the turn-on dv/dt and current spike are much lower with the 5 µm IGBT, which enables the use of lower turn-on gate resistance that results in further reduction of turn-on loss. This makes the 5 µm IGBT more appropriate for higher switching frequency applications. On the other hand, the 2 µm is an ideal choice for lower frequency, higher power applications where the conduction loss is of major concern.

TABLE I: Comparison of 2µm and 5 µm IGBTs

Parameter	2 µm IGBT	5 µm IGBT
Turn-on loss at 8 kV, 5 A	30.4 mJ	30.9 mJ
Turn-off loss at 8 kV, 10 A	12.7 mJ	6.7 mJ
Turn-on current spike magnitude	27 A	11 A
Turn-on dv/dt (at the beginning of the transition)	80 kV/µs	30 kV/µs
Turn-off dv/dt (in the steeper region)	35 kV/µs	28 kV/µs
$R_{G(ON)}$	200 Ω	200 Ω
$R_{G(OFF)}$	10 Ω	10 Ω
Forward drop at 20 A	6 V	7.2 V

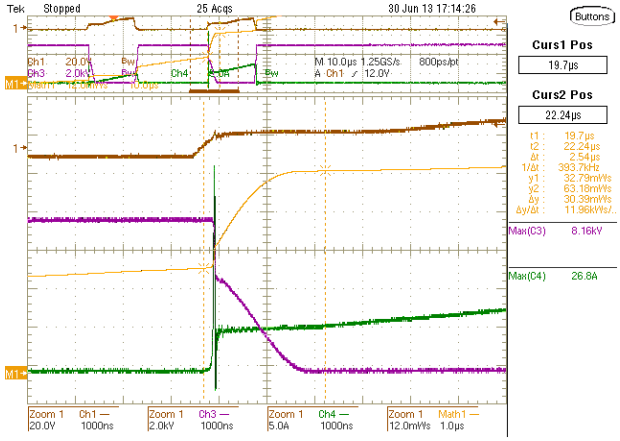

Figure 16: Turn-on transition of 2 µm IGBT at 8 kV, 5 A. [Ch1(Brown): V_{GE} – 20 V/div; Ch3(Magenta): V_{CE} – 2 kV/div; Ch4(Green): I_C – 5 A/div; Math1(Orange): Energy loss – 12 mJ/div; Time scale: 1µs/div].

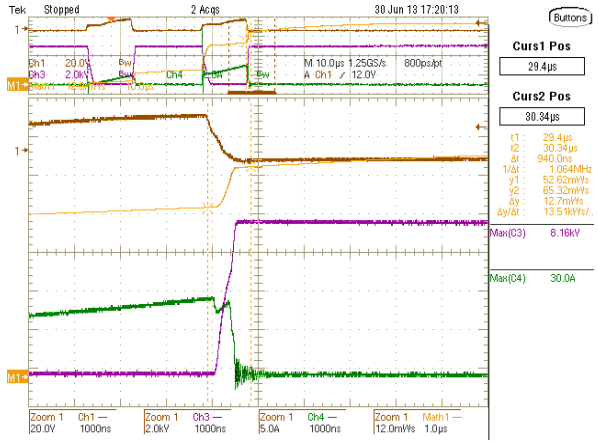

Figure 18: Turn-off transition of 2 µm IGBT at 8 kV, 10 A. [Ch1(Brown): V_{GE} – 20 V/div; Ch3(Magenta): V_{CE} – 2 kV/div; Ch4(Green): I_C – 5 A/div; Math1(Orange): Energy loss – 12 mJ/div; Time scale: 1µs/div].

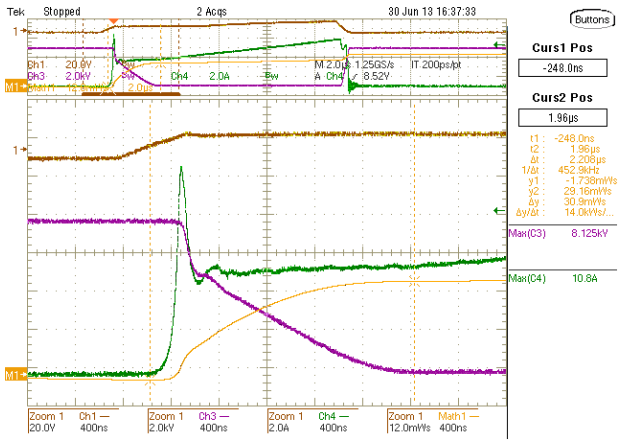

Figure 17: Turn-on transition of 5 µm IGBT at 8 kV, 5 A. [Ch1(Brown): V_{GE} – 20 V/div; Ch3(Magenta): V_{CE} – 2 kV/div; Ch4(Green): I_C – 2 A/div; Math1: Energy loss – 12 mJ/div; Time scale: 400ns/div].

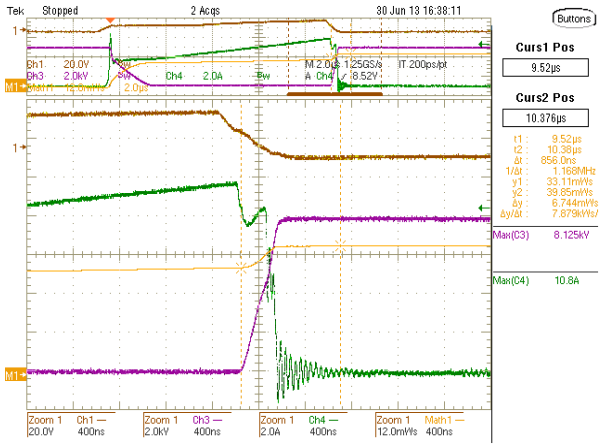

Figure 19: Turn-off transition of 5 µm IGBT at 8 kV, 10 A. [Ch1(Brown): V_{GE} – 20 V/div; Ch3(Magenta): V_{CE} – 2 kV/div; Ch4(Green): I_C – 2 A/div; Math1(Orange): Energy loss – 12 mJ/div; Time scale: 400 ns/div].

VI. Loss Comparison of the SiC IGBTs with SiC MOSFET

In this section, power loss of the 2 µm and 5 µm IGBTs is compared with a MOSFET to consummate the results presented in the earlier sections. The MOSFET with its ratings closer to the IGBTs that was available for this study was a 10 kV, 10 A, Cree SiC MOSFET. However, as there was flexibility in choosing the IGBTs, 12 kV, 10 A IGBTs have been chosen with 2 µm and 5 µm buffer layer thicknesses for this study, to make it a fair comparative evaluation.

Fig. 20 shows turn-on and turn-off transitions of the 10 kV, 10 A MOSFET at 6 kV. The corresponding waveforms for 2 µm and 5 µm IGBTs are shown in Fig. 21 and Fig. 22 respectively. The turn-on current is 4 A and turn-off current is 8 A, and the $R_{G(ON)}$ and $R_{G(OFF)}$ used with all the devices are 100 Ω and 10 Ω respectively. Table II summarizes the corresponding switching data and on-drop at 10 A. The 2 µm and 5 µm have same turn-on loss with 5 µm IGBT with about 60 % lower turn-off loss, as seen with the 15 kV, 20 A IGBTs in the earlier sections. The MOSFET has highest turn-on loss and lowest turn-off loss of all the three devices. The lowest turn-off loss is expected due to unipolar nature of the MOSFET.

It can be seen from the Fig. 20 that the turn-on current spike of the MOSFET is 7.5 A, whereas, the current spike for the 2 µm and 5 µm IGBTs are 24 A and 12.5 A respectively. As the load inductor and the diode used for the tests are same with all the devices, the current spike is an indication of dv/dt produced by the corresponding device. So, ideally, the devices have to be compared with different gate resistances so that the dv/dt produced is same by all of them. This indicates that the 10 kV MOSFET turn-on loss can be considerably reduced by using lower $R_{G(ON)}$ that generates the same current spike (or dv/dt) produced by the 2 µm IGBT. It also implies that the turn-on loss of the 5 µm IGBT can be reduced by using a lower $R_{G(ON)}$, while maintaining the current spike value seen with the 2 µm IGBT.

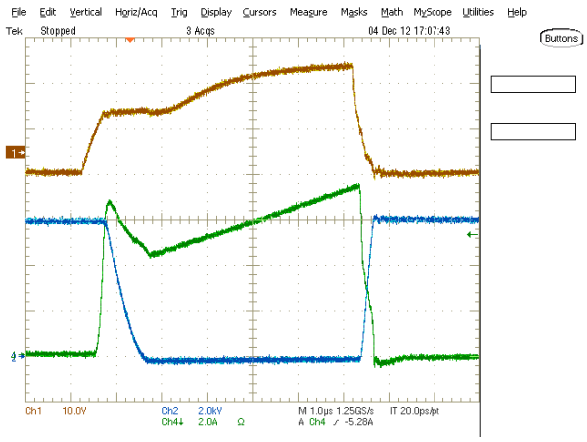

Figure 20: Turn-on and turn off transitions of 10 kV, 10 A SiC MOSFET at 6 kV, 4 A (on) and 8 A (off). [Ch1(Brown): V_{GS} – 10 V/div; Ch2(Blue): V_{DS} – 2 kV/div; Ch4(Green): I_D – 2 A/div; Time: 1 µs/div].

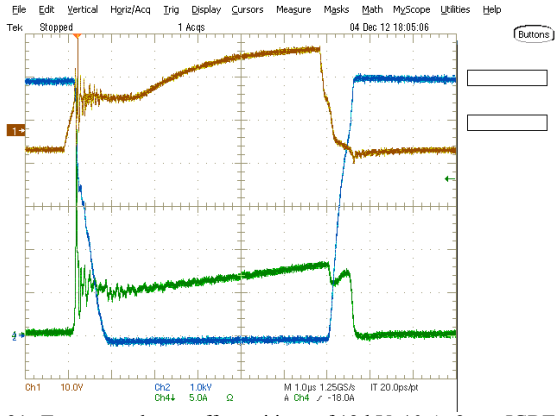

Figure 21: Turn-on and turn-off transitions of 12 kV, 10 A, 2 µm IGBT at 6 kV, 4 A (on) and 8 A (off). [Ch1(Brown): V_{GE} – 10 V/div; Ch2(Blue): V_{CE} – 1 kV/div; Ch4(Green): I_C – 5 A/div; Time: 1 µs/div].

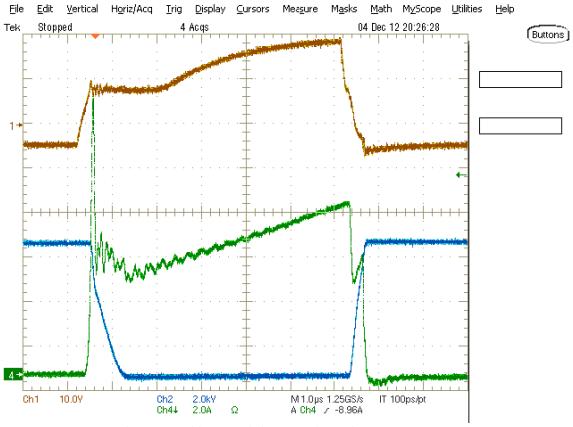

Figure 22: Turn-on and turn-off transitions of 12 kV, 10 A, 5 µm IGBT at 6 kV, 4 A (on) and 8 A (off). [Ch1(Brown): V_{GE} – 10 V/div; Ch2(Blue): V_{CE} – 2 kV/div; Ch4(Green): I_C – 2 A/div; Time: 1 µs/div].

TABLE II: Comparison of the IGBTs with MOSFET

Parameter	10 kV, 10 A MOSFET	12 kV, 10 A, 2 µm IGBT	12 kV, 10 A, 5 µm IGBT
Turn-on loss at 6 kV, 4 A	15.1 mJ	10.7 mJ	10.7 mJ
Turn-off loss at 6 kV, 8 A	1.9 mJ	11.1 mJ	4.4 mJ
Turn-on current spike magnitude	7.5 A	24 A	12.5 A
$R_{G(ON)}$	100 Ω	100 Ω	100 Ω
$R_{G(OFF)}$	10 Ω	10 Ω	10 Ω
Forward drop at 10 A	4.1 V	4.4 V	5.3 V

VII. CONCLUSION

This paper presents characteristics of the state-of-the-art 15 kV SiC n-IGBT. The forward, blocking and switching characteristics along with their temperature dependency are provided. The variation of turn-on and turn-off loss with voltage and current is also given. Then the application benefits of using the ultrahigh voltage IGBT for high power converters and the challenges that are encountered by the power converter designers while using this novel high performance device are discussed. In addition, a comparative analysis of the 2 μm field-stop buffer layer IGBT with a 5 μm buffer layer thickness IGBT is presented with pros and cons of each with respect to the application requirements. Finally, comparison of characteristics of the IGBTs and MOSFET is provided for a complete reference.

ACKNOWLEDGMENT

This work made use of the FREEDM ERC shared facilities supported by the National Science Foundation under Award Number EEC-0812121.

REFERENCES

[1] R. Withanage and N. Shammas, "Series connection of insulated gate bipolar transistors (IGBTs)," IEEE Trans. Power Electron., vol. 27, 2012, pp. 2204-2212.

[2] J. Lai and F. Peng, "Multilevel converters-a new breed of power converters," IEEE Trans. on Ind Applicat., 1996, vol. 32, issue. 3, pp. 509-517.

[3] A. K. Agarwal, "An overview of SiC power devices," International Conf. on Power, Control and Embedded Systems (ICPCES), 2010, pp. 1-4.

[4] M. K. Das, et al., "10 kV, 120 A SiC half H-bridge power MOSFET modules suitable for high frequency, medium voltage applications," Energy Conversion Congress and Exposition (ECCE), 2011, pp. 2689-2692.

[5] R. J. Callanan, et al., " Recent progress in SiC DMOSFETs and JBS diodes at Cree," 34th Annual IEEE Ind. Electronics Conference, 2008, pp. 2885-2890.

[6] Q. Zhang, C. Jonas, S. Ryu, A. Agarwal and J. Palmour, "Design and fabrications of high voltage IGBTs on 4H-SiC," IEEE Int'l Symposium on Power Semiconductor Devices and IC's, ISPSD, 2006, pp. 1-4.

[7] B. J. Baliga, "Advanced high voltage power device concepts," New York: Springer-Verlag, 2012.

[8] S. Ryu, et al., "High performance, ultra high voltage 4H-SiC IGBTs," IEEE Energy Conversion Congress and Exposition (ECCE), 2012, pp. 3603-3608.

[9] B. J. Baliga, "Fundamentals of power semiconductor devices," New York: Springer-Verlag, 2008.

[10] O. D. Patterson and D. M. Divan, "Pseudo-resonant full bridge DC/DC converter," IEEE Transactions on Power Electronics, vol. 6, issue 4, 1991, pp. 671-678.

[11] A. Kadavelugu, et al., "High-frequency design considerations of dual active bridge 1200 V SiC MOSFET DC-DC converter," Applied Power Electronics Conference Congress and Exposition (APEC), 2011, pp. 314-320.